J Mater Sci (2008) 43:7307–7312
DOI 10.1007/s10853-008-2682-2

ULTRAFINE-GRAINED MATERIALS

Formation of ultrafine-grained microstructure in HSLA steel profiles by linear flow splitting

T. Bohn · E. Bruder · C. Müller

Received: 6 March 2008 / Accepted: 25 April 2008 / Published online: 13 July 2008

Abstract Linear flow splitting is a new cold forming process for the production of branched sheet metal structures in integral style. It induces extremely high deformation degrees without formation of cracks in the split sheets due to hydrostatic compressive stresses. Investigations on a HSLA steel (ZStE 500) show the formation and fragmentation of a dislocation cell structure in the severely deformed regions of the steel sheet. This results in ultrafine-grained microstructures and improved mechanical properties, similar to SPD processes as Equal Channel Angular Pressing (ECAP) or High Pressure Torsion (HPT). EBSD measurements reveal a gradient in grain size with an increase in direction perpendicular to the surface, whereas micro hardness decreases in the same direction. Based on these results, basic principles of linear flow splitting and its expected potential are discussed.

Introduction

The global competition and the limited material resources force companies to increase their product functionality as well as to optimize the manufacturing cycles. This involves an increased complexity of the products and simultaneously enforces improvements of the manufacturing technologies. The requirements on the material properties are increasing continuously. Preferably materials would be used whose high performances do not limit the production process by exhausted formability. Therefore UltraFine Grained (UFG) microstructures with grain dimensions in the submicron range, characterized by high mechanical strength as well as high ductility, are of great economic and scientific interest [1]. Presently UFG materials are manufactured by several methods of Severe Plastic Deformation (SPD), like Equal Channel Angular Pressing (ECAP) [2], Accumulative Roll Bonding (ARB) [3], and High Pressure Torsion (HPT) [4]. All these SPD methods are characterized by high hydrostatic compression stresses, which enable extremely high deformations in the work piece. Cells, cellblocks, and microbands are formed within the grains and a subgrain structure of Low Angle Grain Boundaries (LAGBs) is created. With further deformation the LAGBs develop to High Angle Grain Boundaries (HAGBs) and lead to a grain refinement with grain sizes in the submicron range [5, 6]. The typical strains to generate homogeneous UFG microstructures with a majority fraction of HAGBs is about $\varepsilon = 4$–8 [3, 5, 7], depending on the method and the material, respectively. Originally, these processes were developed for fundamental investigations [1, 8, 9], but due to their excellent properties an interest for the industrial utilization of UFG metals processed by SPD evolved, especially for aerospace and medical applications.

The new linear flow splitting technology is a process where such a microstructure appears in real components. Here, the edge of a sheet metal (sheet or coil) is formed into two flanges by splitting and supporting rolls. Bifurcated sheet metal components without lamination of material are produced (Fig. 1) and can be roll formed afterward and welded to generate multi-chambered profiles [10, 11]. These profiles are characterized by strongly inhomogeneous deformation resulting in microstructural and property gradients that are not characterized yet. The present article gives more insight in the specific

T. Bohn (✉) · E. Bruder · C. Müller
Division Physical Metallurgy, Materials Science, Technische Universität Darmstadt, Petersenstr. 23, D-64287 Darmstadt, Germany
e-mail: t.bohn@phm.tu-darmstadt.de

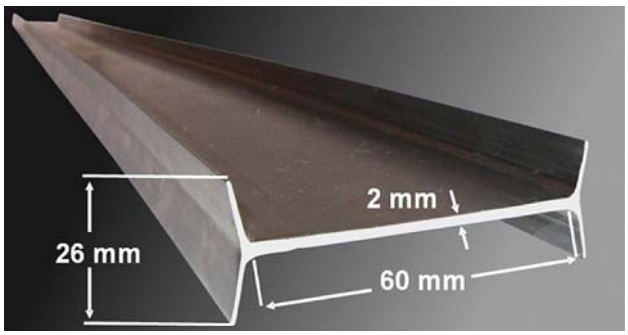

Fig. 1 Profile produced by linear flow splitting

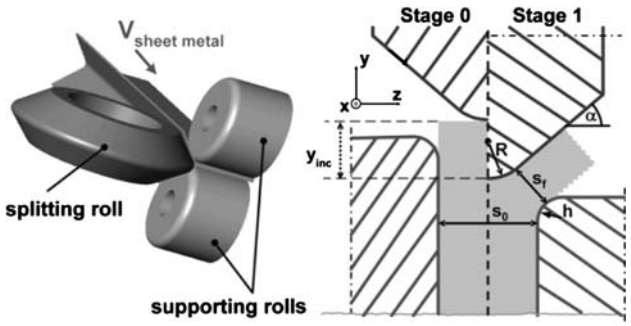

Fig. 2 Principle of linear flow splitting

deformation process and highlights the resulting microstructure as well as local and global properties of profiles produced by linear flow splitting.

Principle of linear flow splitting

Linear flow splitting is a new cold forming process for the production of bifurcated integral profiles from sheet metal. The tooling system consists of an obtuse angled splitting roll and two supporting rolls (Fig. 2). The final profile geometry originates from several discrete forming steps in which the splitting roll drives into the band edge by an incremental splitting depth (y_{inc}). High hydrostatic stresses in the processing zone prevent the formation of cracks and allow a high total splitting depth (y_{tot}). Linear flow splitting can be conducted either in a reversing process with a single roll stand or integrated in a mill train for continuous processing. Further details on the process principle and possible applications are presented elsewhere [10, 11].

Experimental

The material used in this investigation is a HSLA steel sheet of the grade ZStE 500 (0.07 wt.% C, 0.71 wt.% Mn, 0.1 wt.% Cr, 0.047 wt.% Si, 0.034 wt.% Nb and 0.016 wt.% Al), designed for deep drawing. Linear flow splitting was conducted at the Institute for Production Engineering and Forming Machines (Technische Universität Darmstadt) in a reversing process to a total splitting depth (y_{tot}) of 20 mm with an incremental splitting depth (y_{inc}) of 1 mm, a flange thickness (s_f) of $\sim$1 mm and an angle of the flanges (α) of 10°. Shape and dimensions of the resulting profiles are shown in Fig. 1.

Metallographic specimens were prepared from the cross section of the profiles. For EBSD (Electron BackScatter Diffraction) measurements the specimens were vibropolished for at least 8 h on a 50 nm mixed oxide suspension. EBSD measurements were carried out using a FEG SEM

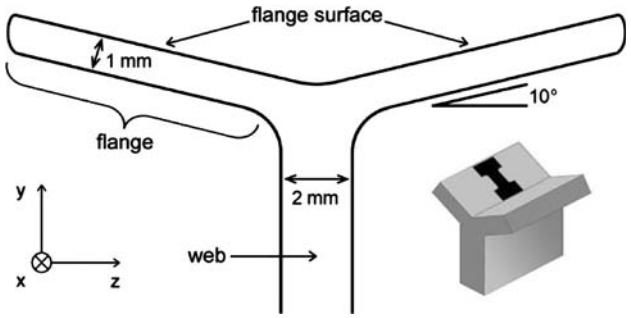

Fig. 3 Profile scheme

fitted with a TSL EBSD system. LAGBs have been defined between 2° and 15° misorientation and HAGBs above a misorientation of 15°.

Hardness measurements (HV0,05) were performed on the cross section of the profile from the splitting center to the web and parallel to the flange surface, Fig. 3.

Tensile specimens were machined from the as received material as well as from the flanges in transverse direction (Fig. 3). The gage length was 3 mm with a width of 2 mm. Specimens were machined only on the lower side of the flange to a thickness of 0.8 mm.

Results

Microstructure

The microstructure of the as received HSLA steel consists of equiaxed ferrite grains with small cementite precipitations located at the grain boundaries. The average grain size of the sheet material measured by optical microscopy was $\sim$6 µm (Fig. 4).

In the highly deformed regions, i.e., the splitting center and the flange surface, the microstructure cannot be resolved by light microscope. EBSD measurements reveal that linear flow splitting leads to an UFG microstructure in the splitting center and accordingly the flange surface area. Due to the preferential flow direction of the material

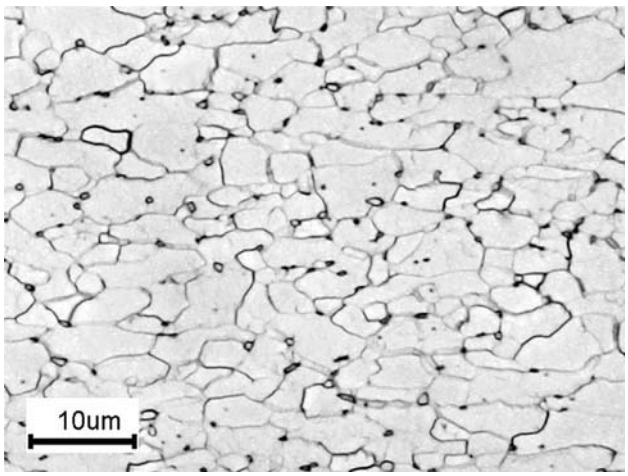

Fig. 4 Microstructure of the as received material

(perpendicular to the splitting direction) a pancake like UFG microstructure develops, thus the grain dimensions in the flanges are strongly dependent on the direction, which is exemplarily shown in Fig. 5 for a position 50 µm underneath the flange surface. The maximum grain dimensions are parallel to the z-axis and the minimum parallel to the y-axis. The following micrographs concentrate on the y × z plane as it includes these two directions. Note that although the structure in the x × z plane is comparatively coarse its area-related average grain size is still less than 1 µm.

Detailed investigations on the microstructure of the as rolled flanges reveal a grain size gradient perpendicular to the flange surface which is presented in Fig. 6 by EBSD maps (combined image quality + inverse pole figure). The elongated grains near the surface are mostly separated by HAGBs and show only marginal fragmentation. Within 50 µm to the flange surface the average grain dimensions along the y-axis (line intersection perpendicular to the split

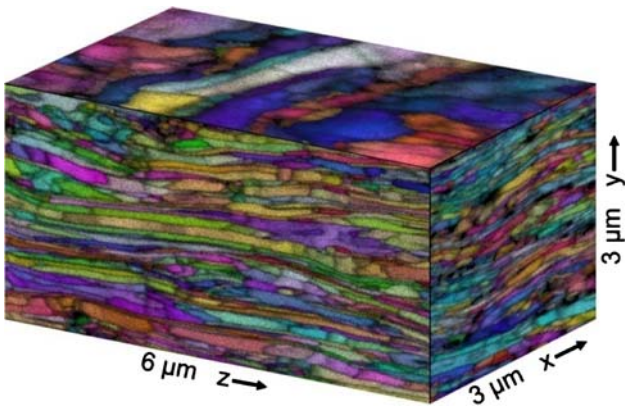

Fig. 5 EBSD maps (image quality + inverse pole figure) of the planes perpendicular to the x-, y-, and z-axis 50 µm underneath the flange surface

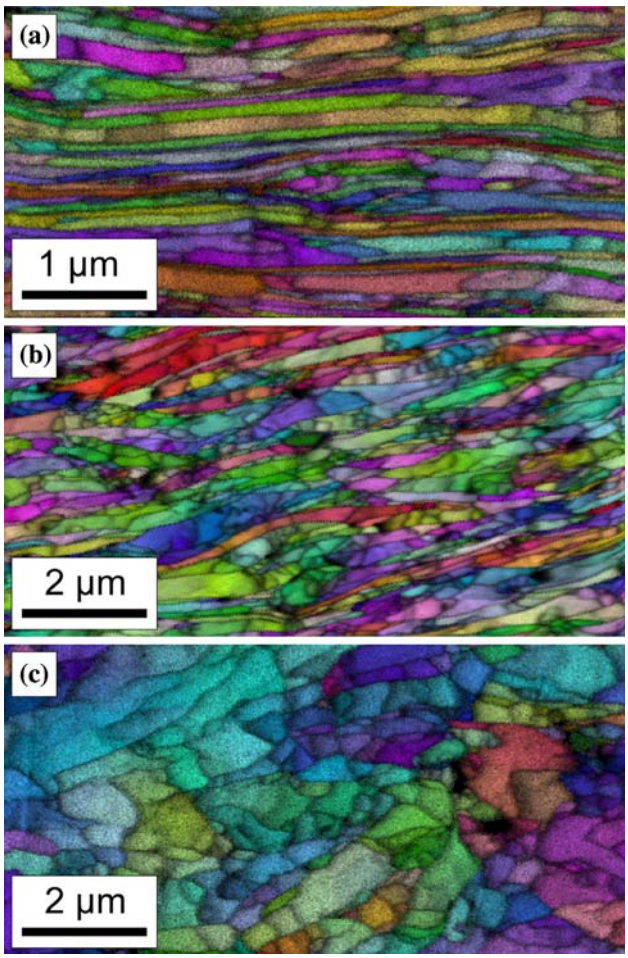

Fig. 6 EBSD maps (image quality + inverse pole figure) with different distances to the flange surface: (**a**) 50 µm, (**b**) 250 µm, and (**c**) 550 µm

surface) are below 100 nm. With increasing depth, i.e., distance to the split surface, the grain structure becomes coarser and more equiaxed. The average grain size (linear intersection) increases with growing distance to the flange surface and reaches a value of approximately 500 nm at a depth of 700 µm. This coarsening is associated with a decreasing fraction of HAGBs from over 80% close to the flange surface to about 30% at the lower side of the flange (Fig. 7). No microstructural gradients are observed along the splitting direction and parallel to the flanges (except at the flange tip, about 4 mm in length). Thus Figs. 5–7 are representative for a large part of the flanges.

The distribution of HAGBs and LAGBs with different distances to the splitting center is illustrated in Fig. 8, on the basis of EBSD maps (inverse pole figure) with marked grain boundaries. HAGBs are traced in black and LAGBs in white. Figure 8a (650 µm below slitting center) shows that the HAGBs primarily separate regions with a few microns in diameter, which is about the grain size of the initial sheet material. These regions are further fragmented

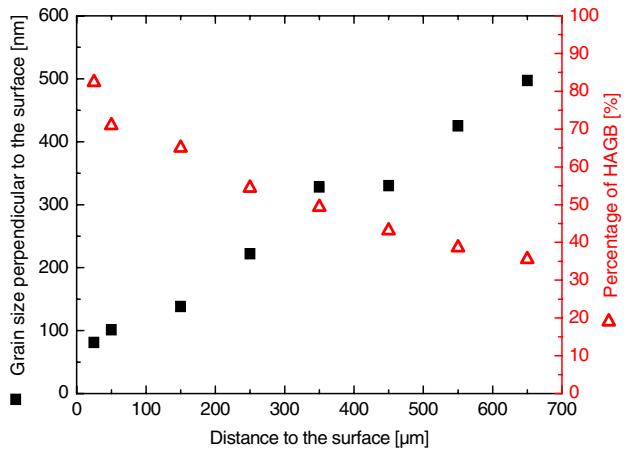

Fig. 7 Grain dimensions perpendicular to the surface and HAGB fraction versus distance to the surface

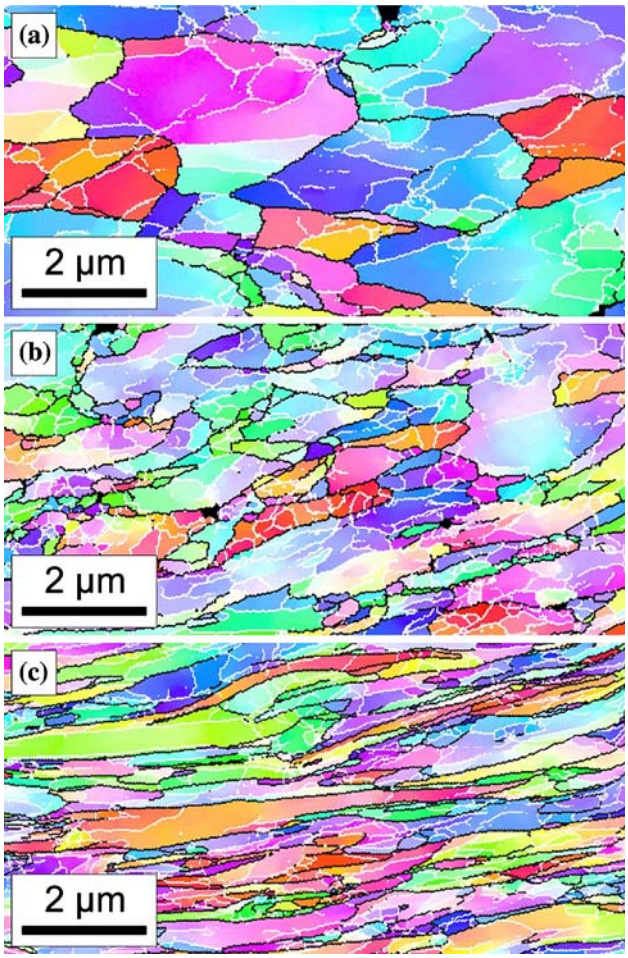

Fig. 8 EBSD maps of the processing zone (inverse pole figure + marked grain boundaries) with different distances to the splitting center: (**a**) 650 µm, (**b**) 450 µm, and (**c**) 250 µm

by a dislocation cell structure, i.e., a network of LAGBs with a sub-micron cell size. Comparing Fig. 8a and b reveals a refinement of the cell structure with decreasing distance to the surface. The misorientation between adjacent cells thereby increases, thus 15° of misorientation are exceeded by an increasing fraction. The resemblance between the HAGBs and the initial coarse-grained microstructure in Fig. 8a is no more observable within 500 µm to the splitting center (see Fig. 8b, c). In this region the HAGBs predominantly form a banded structure parallel to the flange surface that is further subdivided by HAGBs and LAGBs. The spacing between the banded HAGBs decreases towards the flange surface as well as the transverse fragmentation of the elongated structure.

Mechanical properties

The average hardness of the as received material was measured to 196 HV0.05 and is homogeneous across the cross section. Hardness measurements on split flanges from the splitting center to the flange tips (25 µm below the surface) reveal a constant hardness of 365 HV0.05 parallel to the surface over a wide range of the flange in spite of the altering deformation degree along the flange surface. Only at the flange tips, i.e., the surface created at the first splitting steps, the expected correlation—decreasing hardness with decreasing deformation—can be observed.

The split profile shows a steep hardness gradient from the surface of the splitting center to the web. The highest hardness is measured at the surface with a value of 365 HV0.05. With increasing distance to the surface the hardness decreases and reaches a constant level in a depth of 1 mm of 225 HV0.05, which is about 30 HV0.05 higher than the as received material, Fig. 9. The same behavior (identical hardness distribution) was found for the whole zone of constant hardness in Fig. 10.

Tensile tests reveal an increase in yield and tensile strength (744 MPa and 782 MPa) of about 60% in the

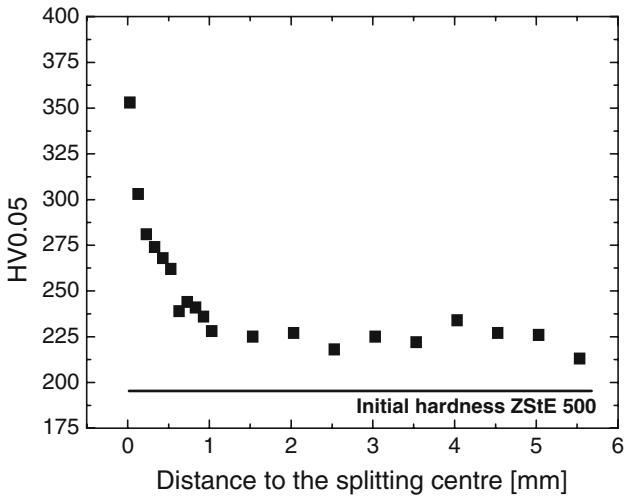

Fig. 9 Hardness repartition from the splitting center to the web

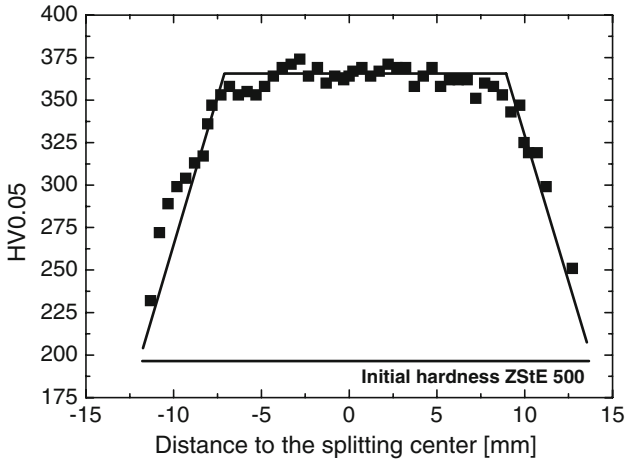

Fig. 10 Hardness repartition parallel to the flange surface 25 μm underneath the surface

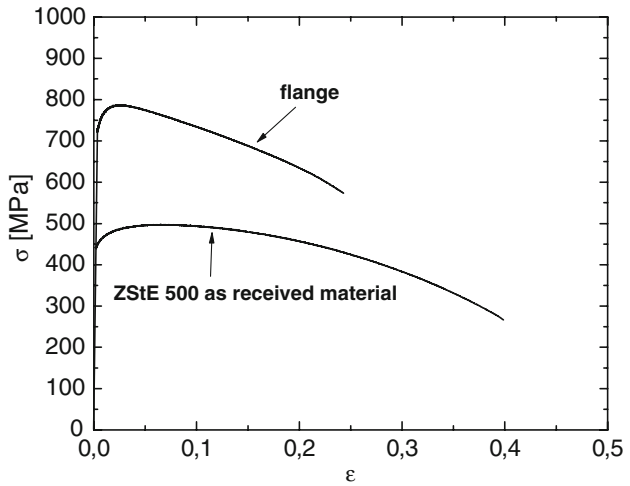

Fig. 11 Engineering stress–strain curves of as received and flange material

flanges compared to the as received material (Fig. 11). The increased strength is associated with a reduced fracture strain and marginal uniform elongation as it is typical for UFG microstructures. Note that due to the samples thickness (0.8 μm) the tensile specimens include a microstructural and hardness gradient perpendicular to the loading direction. In loading direction as well as in direction of the specimen width microstructure and hardness are constant, respectively.

Discussion

Linear Flow splitting is characterized by complex deformation and flow processes of the material. To get a better insight into these processes it is advantageous to separate the split profile in two zones: The process zone where the UFG microstructures develop and the flange zone where no further deformation takes place. The process zone is roughly limited by the area within a triangle between the contact points of the splitting and the supporting rolls with the sheet material. In this volume high hydrostatic compressive stresses are present and increase the formability of the material to a degree that UFG microstructures can develop. Even though quantitative descriptions of the strain distribution in the process zone are difficult, it is certainly reasonable to assume a decreasing deformation degree in direction from the splitting roll to the web. Hence, microstructural observations in this direction allow describing the evolution of the microstructure as a function of deformation. The EBSD measurements performed in this project show the transition from a dislocation cell structure into an UFG pancake microstructure with increasing deformation. At first a dislocation cell structure with low angles of misorientation is formed within the initial grain boundaries. The cell spacing decreases with further deformation while the misorientation increases thus partially forming new HAGBs. Subsequently the microstructure transforms into a banded structure with an increasing aspect ratio due to the preferential flow direction of the material. The cells are increasingly refined and mostly separated by HAGBs. This results in a fraction of more than 80% HAGBs and average grain dimensions below 100 nm (perpendicular to the surface) in the most severely deformed regions close to the splitting center.

The flange zone where no further deformation takes place represents the microstructural evolution of previous splitting steps, i.e., of previous processing zones. Therefore it is not surprising to find similarities to the observations mentioned above for the process zone: UFG microstructures with a grain size gradient perpendicular to the flange surface combined with a hardness gradient due to the changing grain size. However the constant hardness parallel to the surface over a wide range of the flange (Fig. 10) is surprising at first glance, as FEM modeling clearly indicates an increasing deformation degree towards the splitting center [10, 12]. By the microstructural evolution, i.e., the formation of UFG microstructures in the process zone this effect becomes plausible. As it is well known for SPD processes like ECAP or HPT, UFG microstructures and mechanical properties become almost independent of further deformation when a certain strain is exceeded [4, 7, 13]. In this case increasing deformation is no more coupled with an increasing hardness. In the HSLA steel used for the present investigations this strain is reached at a flange length of about 4 mm, where the zone of constant hardness starts. EBSD measurements reveal constant microstructural dimensions over the whole range of constant hardness, thus microstructure and hardness in the flange become identical to those in the processing zone of the split profile. From

these results it can be concluded, that at a flange length of about 4 mm a steady-state is reached in the processing zone. The steady-state in the process zone has two important consequences:

1. Microstructural and property gradients are limited to the direction perpendicular to the flange surface (except the flange tips).
2. Further splitting becomes possible, no limitation of the splitting due to limited formability is expected for the HSLA Steel. From these findings the question arises, whether reaching this steady-state achievable by the formation of UFG microstructures is even a mandatory condition for the flow splitting process.

Due to the formation of UFG microstructures the flanges show excellent mechanical properties. Stress–strain curves of specimen taken parallel to the flanges display the typical shape of UFG microstructures: High yield stress, little work hardening, little uniform elongation but high fracture strain [9, 14–16]. As the tensile specimen contains a grain size gradient in thickness direction, the yield stress in the surface area is even higher than 744 MPa measured on the sample. An estimation on the basis of hardness measurements [12] reveals a value above 1,000 MPa in the surface area of the flanges. This extremely high yield stress makes the profile especially interesting for applications where high wear resistance and good fatigue properties are required.

Summary and conclusion

The HSLA steel ZStE 500 was used to investigate the microstructure and mechanical properties of bifurcated profiles produced by linear flow splitting.

Linear flow splitting leads to the formation of UFG microstructures at the surface area of the split flanges. The UFG microstructure develops by the formation and fragmentation of a dislocation cells. The resulting grain size decreases with increasing deformation and the fraction of HAGB increases. This leads to a process characteristic ultrafine grain size gradient perpendicular to the split surface.

Due to the formation of UFG microstructures a steady-state is reached in the process zone, where increasing deformation (i.e., splitting depth) has no more or little influence on microstructure and resulting properties. Thus work hardening and the related reduction of formability are no limiting parameters for the splitting process.

The flanges exhibit very high yield stress combined with an acceptable ductility. Hardness and yield stress gradients perpendicular to the split surface are a consequence of the process characteristic microstructure.

Acknowledgements The investigations presented in this article are supported by the German Research Foundation (DFG). The authors thank the DFG for funding the subproject C1 of the Collaborative Research Center 666 “Integral sheet metal design with higher order bifurcations—Development, Production, Evaluation”.

References

1. Valiev RZ, Estrin Y, Horita Z, Langdon TG, Zehetbauer MJ, Zhu YT (2006) JOM 58:33. doi:10.1007/s11837-006-0213-7
2. Furukawa M, Horita Z, Nemoto M, Langdon TG (2001) J Mater Sci 36:2835. doi:10.1023/A:1017932417043
3. Tsuji N, Saito Y, Utsunomiya Y, Tanigawa S (1999) Scripta Mater 40:795
4. Zhilyaev AP, Nurislamova GV, Kim B-K, Baró MD, Szpunar JA, Langdon TG (2003) Acta Mater 51:753. doi:10.1016/S1359-6454(02)00466-4
5. Iwahashi Y, Horita Z, Nemoto M, Langdon TG (1997) Acta Mater 45:4733. doi:10.1016/S1359-6454(97)00100-6
6. Hughes DA, Hansen N (1997) Acta Mater 45:3871. doi:10.1016/S1359-6454(97)00027-X
7. Pragnell PB, Bowen JR, Gholinia A (2001) In: Dinesen AR, Eldrup M, Juul Jensen D, Linderoth S, Pederson TB, Pryds NH, Schrøder Pedersen A, Wert JA (eds) Proceedings of the 22nd Risø international symposium on materials science, Risø National Laboratory, Roskilde, Denmark, p 105
8. Zhu YT, Lowe TC, Langdon TG (2004) Scripta Mater 51:825. doi:10.1016/j.scriptamat.2004.05.006
9. Valiev RZ, Islamgaliev RK, Alexandrov IV (2000) Prog Mater Sci 45:103. doi:10.1016/S0079-6425(99)00007-9
10. Groche P, Vucic D, Jöckel M (2007) J Mater Process Technol 183:249. doi:10.1016/j.jmatprotec.2006.10.023
11. Groche P, Ringler J, Vucic D (2007) Key Eng Mater 344:251
12. Müller C, Bohn T, Bruder E, Bruder T, Landersheim V, el Dsoki C, Groche P, Veleva D (2007) Mat-wiss u Werkstofftech 38:842. doi:10.1002/mawe.200700210
13. Kim HS, Ryu WS, Janecek M, Baik SC, Estrin Y (2005) Adv Eng Mater 7:43. doi:10.1002/adem.200400146
14. Tsuji N, Ito Y, Saito Y, Minamino Y (2002) Scripta Mater 47:893. doi:10.1016/S1359-6462(02)00282-8
15. Wang YM, Ma E (2004) Mater Sci Eng A 375–377:46
16. Shin DH, Park K-T (2005) Mater Sci Eng A 410–411:299